A POROVISCOHYPERELASTIC MODEL FOR NUMERICAL ANALYSIS OF MECHANICAL BEHAVIOR OF SINGLE CHONDROCYTE

Trung Dung Nguyen, Adekunle Oloyede, and Yuantong Gu*
School of Chemistry, Physics and Mechanical Engineering, Science and Engineering Faculty, Queensland University of Technology, Brisbane, Queensland, Australia

The aim of this paper is to utilize a poroviscohyperelastic (PVHE) model which is developed based on the porohyperelastic (PHE) model to explore the mechanical deformation properties of single chondrocytes. Both creep and relaxation responses are investigated by using FEM models of micropipette aspiration and AFM experiments, respectively. The newly developed PVHE model is compared thoroughly with the SnHS and PHE models. It has been found that the PVHE can accurately capture both creep and stress relaxation behaviors of chondrocytes better than other two models. Hence, the PVHE is a promising model to investigate mechanical properties of single chondrocytes.

Keywords: Porohyperelastic, poroviscohyperelastic, chondrocyte, finite element analysis, biomechanics.

I. Introduction

Articular cartilage is the flexible soft tissue that lines the surfaces of the diarthrodial joints to provide a low-friction load-bearing surface in order to avoid large stress exerting on the bones during deformations (Mow, Ratcliffe, & Poole, 1992; Oloyede, Flachsmann, & Broom, 1992). Chondrocytes are the mature cells which perform several functions within the cartilage. The alteration of the mechanical properties of chondrocytes is considered to be one of the main causes of osteoarthritis (Jones et al., 1997; Trickey, Lee, & Guilak, 2000). Therefore, studying the mechanical properties and behavior of individual chondrocytes will help us to understand the role of mechanical loads in accelerating tissue regeneration or degeneration. This could offer insights into new therapies to decrease the effects of osteoarthritis.

In the literature, there are a number of new experimental techniques have been developed to quantitatively characterize the mechanical properties of living cells. Among these methods, Atomic Force Microscopy (AFM) is an advanced technique that is capable of high resolution imaging of tissues, cells and any surfaces as well as

determining mechanical properties of the samples (Faria et al., 2008; Kuznetsova, Starodubtseva, Yegorenkov, Chizhik, & Zhanov, 2007; Lin, Dimitriadis, & Horkay, 2007; Rico et al., 2005; Touhami, Nysten, & Dufrene, 2003; Zhang & Zhang, 2007). Recently, this powerful technique has been more and more extensively utilizing for cell mechanics studies (Darling, Zauscher, Block, & Guilak, 2007; Darling, Zauscher, & Guilak, 2006; Franz & Puech, 2008; Kuznetsova et al., 2007).

There are a number of continuum mechanical models have been proposed in the literature to investigate the mechanical behavior of single cells as well as soft tissues. Poroelastic model which is fundamental for Soil Mechanics is one of the models (Biot, 1941; Terzaghi, 1943). This model has been improved and applied to cartilage which is a biological tissue (Higginson & Norman, 1974; McCutchen, 1982, 1998; Oloyede & Broom, 1991, 1996). This poroelastic model assumes soft tissues as consisting of an incompressible deformable porous elastic solid skeleton that is saturated by an incompressible mobile fluid. This continuum model has been extended to a porohyperelastic (PHE) material law to account for non-linear behavior of material (Simon & Gaballa, 1989). PHE model have been applied in a variety of biomechanical studies yielding reasonable and acceptable results. With this approach, it would provide us with a clear insight into the consolidation as well as swelling behaviors of the cell. Although the PHE model has been extensively and effectively utilized in tissue engineering e.g. articular cartilage (Oloyede & Broom, 1991, 1996), there is lack of research striving to apply this model in modeling single living cell.

It is hypothesized that the behaviors of chondrocytes are influenced by not only the interaction between solid and fluid components but also the intrinsic viscoelasticity of solid components (Baaijens, Trickey, Laursen, & Guilak, 2005; Mow, Kuei, Lai, & Armstrong, 1980; Shieh, Koay, & Athanasiou, 2006; Trickey, Baaijens, Laursen, Alexopoulos, & Guilak, 2006). Thus, in this paper, the poroviscohyperelastic (PVHE) model is developed based on the PHE model to explore the mechanical deformation properties of single chondrocytes. Both creep and relaxation responses are investigated by using FEM models of micropipette aspiration and AFM experiments, respectively. Despite of many advances, to our knowledge, the PVHE model has not been used widely for studying living cell mechanics particularly chondrocyte. Thus, this study

would be the first one to use this PVHE model for chondrocytes with FEM as a simulation tool.

Briefly, the aim of this study is to explore the mechanical deformation behavior of a single chondrocyte such as creep and stress relaxation responses using a computational approach based on FEM simulations. The stress relaxation simulation of chondrocytes will be validated with AFM stress relaxation experiments. The newly developed PVHE model is compared thoroughly with the Standard Neo-Hookean Solid (SnHS) and PHE models. The creep behavior is then investigated by simulating the micropipette aspiration experiments.

II. Materials and Models

2.1. Sample preparation and AFM set-up

The chondrocytes in this study were cultured using similar protocol to previous work (Singh, Jones, Crawford, & Xiao, 2008). After culturing, the cells were trypsinized and seeded onto poly-D-lysine (PDL, Sigma-Aldrich) coated cultured petri dish for 1-2h. AFM system used was a JPK NanoWizard II AFM (JPK Instruments, Germany). A triangular colloidal probe CP-PNPL-BSG-A-5 (NanoAndMore GMBH) cantilever, of which spring constant was determined to be 0.0217 N/m using the thermal noise fluctuations, was used in the experiments. The colloidal probe has a diameter of 5 μm (see Figure 1). Single chondrocytes were indented at the velocity of 13 μm/s and allowed to relax for 60 seconds after indentation (see Figure 2 for details). The force-indentation and force-time curves were then extracted and analyzed using JPKSPM data processing software version 4.4.23 (JPK Instruments, Germany).

2.2. Continuum mechanical models for the single cell

2.2.1. Standard Neo-Hookean Solid (SnHS) model

This SnHS model assumes the cell to be a homogenous solid-like material. In the differential form of linear viscoelasticity, the stress is expressed in terms of strain history with three material constants i.e. k_1, k_2 and μ (Zhou, Lim, & Quek, 2005):

$$\mathbf{S} + \frac{\mu}{k_2}\dot{\mathbf{S}} = k_1\varepsilon + \mu\left(1 + \frac{k_1}{k_2}\right)\dot{\varepsilon} \quad (1)$$

$$\varepsilon = \nabla\mathbf{u} + \nabla\mathbf{u}^T \qquad \dot{\varepsilon} = \nabla\mathbf{v} + \nabla\mathbf{v}^T \qquad \mathbf{S} = \sigma + p\mathbf{I} \quad (2)$$

where **S** is the deviatoric stress tensor, **ε** is the engineering strain tensor, which is the same as the deviatoric component under the condition of incompressibility, $\dot{\boldsymbol{\varepsilon}}$ is the engineering strain rate tensor (the superposed dot denotes differentiation with respect to time), k_1 and k_2 are two elastic constants, μ is a viscous constant (see Figure 3c)**, u** is the displacement field, **v** is the velocity field, **σ** is the total stress tensor, p is the hydrostatic pressure and **I** is the unit tensor.

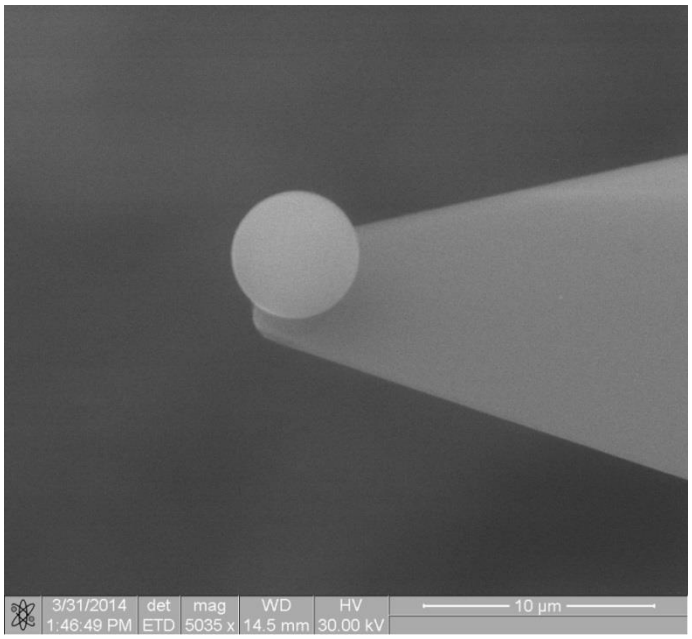

Figure 1 SEM image of a colloidal probe cantilever

In 2005, (Zhou et al., 2005) proposed a nonlinear viscoelastic model, namely, the Standard Neo-Hookean Solid (SnHS) model for the large deformation analysis of living cells, and is an extension of the Standar Linear Solid (SLS) viscoelasticity model. This model replaced the linear elasticity elements by Neo-Hookean hyperelastic elements, leading to a simple constitutive law, where the strain energy density function of the incompressible material is:

$$U = \frac{G_0}{2}(I_1 - 3) \quad (3)$$

where G_0 is the shear modulus, I_1 is the first deviatoric strain invariant, defined as:

$$I_1 = \lambda_1^2 + \lambda_2^2 + \lambda_3^2 \tag{4}$$

With λ_1, λ_2 and λ_3 being deviatoric stretches. The deviatoric part **S** of the Cauchy stress tensor is:

$$\begin{aligned} \mathbf{S} &= G_0\left(\mathbf{B} - \frac{1}{3}I_1.\mathbf{I}\right) \\ \mathbf{B} &= \mathbf{F}.\mathbf{F}^T \qquad \mathbf{F} = \frac{\partial \mathbf{x}}{\partial \mathbf{X}} \end{aligned} \tag{5}$$

where **S** is the deviatoric part of the Cauchy stress tensor, **F** is the deformation gradient of the current configuration **x** relative to the initial configuration **X**, and **B** is the left Cauchy-Green strain tensor.

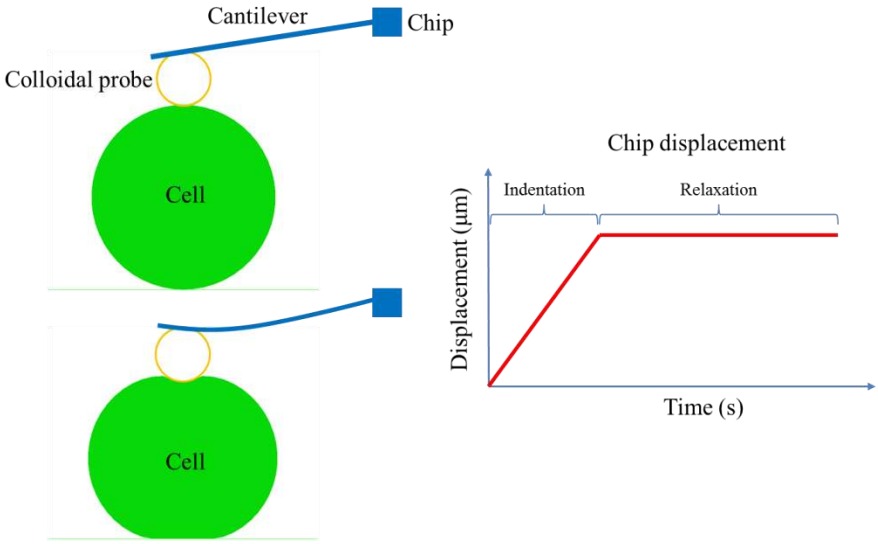

Figure 2 AFM relaxation test diagram. A colloidal probe indented the cell using a step displacement, which was then kept constant to study relaxation behavior of single cells

The shear relaxation modulus $G(t)$ can be expressed as a Prony series expansion with the first term:

$$G(t) = G_0\left[1 - g_1\left(1 - e^{-t/\tau_1}\right)\right] \tag{6}$$

where g_1 and τ_1 are material constants.

This deviatoric part of the Cauchy stress tensor can further be written as:

$$\mathbf{S}(t) = \mathbf{S}_0(t) + \mathrm{SYM}\left[\int_0^t \frac{\dot{G}(s)}{G_0}\mathbf{F}_t^{-1}(t-s).\mathbf{S}_0(t-s).\mathbf{F}_t(t-s)ds\right] \tag{7}$$

$$\mathbf{F}_t(t-s) = \frac{\partial \mathbf{x}(t-s)}{\partial \mathbf{x}(t)}$$

where $\mathbf{F}_t(t-s)$ is the deformation gradient of the configuration $\mathbf{x}(t-s)$ at time $t-s$, relative to the configuration $\mathbf{x}(t)$ at time t , and $\mathbf{S}_0(t)$ represents the instantaneous stress caused by the deformation, which can be computed using Eq. (5), SYM[·] denotes the symmetric part of the matrix.

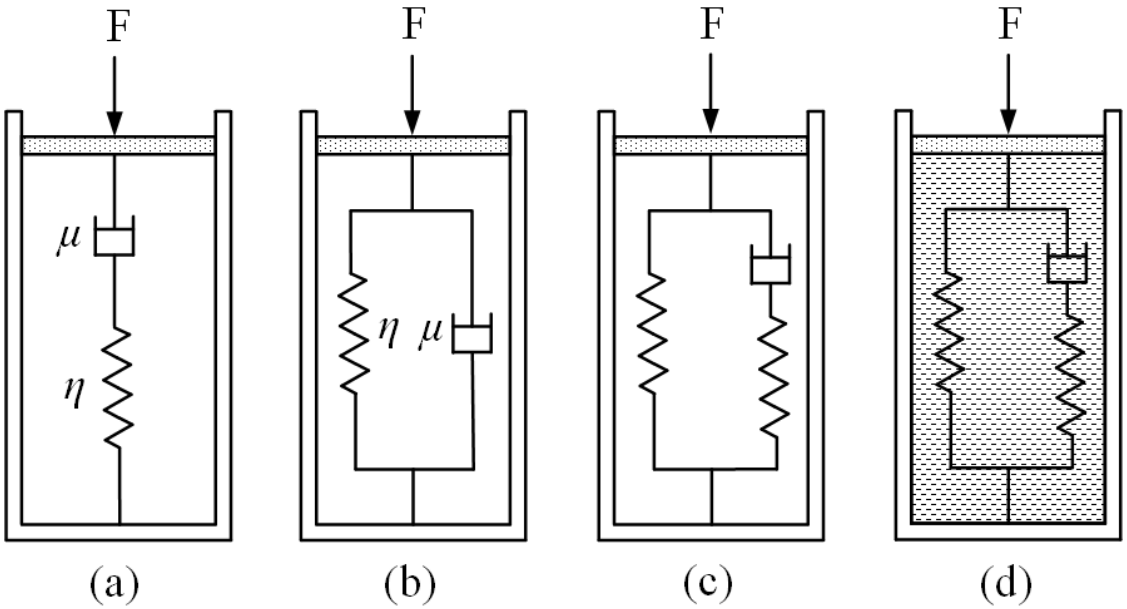

Figure 3 Models of linear viscoelasticity: (a) Maxwell, (b) Voigt, (c) Standard linear solid, and (d) PVHE model

2.2.2. Porohyperelastic (PHE) field theory

In order to characterise and predict the finite strain and non-linear responses of structures, the porohyperelastic PHE theory was developed as an extension of poroelastic theory (Simon & Gaballa, 1989). This theory assumes that the chondrocyte is a continuum consisting of an incompressible hyperelastic porous solid skeleton saturated by an incompressible mobile fluid. Even though both solid and fluid are incompressible, the whole cell is compressible because of the volume loss of fluid during deformation. It has been applied in many engineering fields including Soil Mechanics (Sherwood, 1993) and Biomechanics (Meroi, Natali, & Schrefler, 1999; Nguyen, 2005; Simon, 1992). The details of this theory are described clearly in the literature (Kaufmann, 1996; Simon, 1992; Simon, Kaufmann, McAfee, & Baldwin, 1998; Simon, Kaufmann, McAfee, Baldwin, & Wilson, 1998; Simon, Liable, Pflaster,

Yuan, & Krag, 1996). A summary of field equations for the isotropic form of this theory is stated below:

Conservation of linear momentum:

$$(\partial T_{ij})/(\partial X_j) = 0 \tag{8}$$

Conservation of fluid mass (Dacy's law):

$$\tilde{k}_{ij} \frac{\partial \pi^f}{\partial X_i} = \dot{\tilde{w}}_j \tag{9}$$

Conservation of (incompressible) solid and (incompressible) fluid mass is a constraint of the form:

$$\frac{\partial \dot{\tilde{w}}_i}{\partial X_k} + J H_{kl} \dot{E}_{kl} = 0 \tag{10}$$

Where the constitutive law:

$$\sigma_{ij} = \sigma^e_{ij} + \pi^f \delta_{ij}, \quad \sigma^e_{ij} = J^{-1} F_{im} S^e_{mn} F_{jn} \tag{11}$$

$$S_{ij} = S^e_{ij} + J \pi^f H_{ij}, \quad S^e_{ij} = \frac{\partial W^e}{\partial E_{ij}} \tag{12}$$

where T_{ij}, π^f, $\tilde{k}_{ij}$, $\tilde{w}_j$, H_{ij}, S^e_{ij} and W^e are first Piola-Kirchhoff total stress, fluid stress, symmetric permeability tensor, Lagrangian fluid velocity, Finger's strain, second Piola-Kirchhoff stress and effective strain energy density function, respectively. For simplicity, the Neo-Hookean strain energy density function would be used in this study.

The hydraulic permeability of osteocyte was assumed to be strain dependent and be a function of void ratio for the finite element simulations (Wu & Herzog, 2000):

$$k = k_0 \left(\frac{e}{e_0}\right)^{\kappa} exp\left\{\frac{M}{2}\left[\left(\frac{1+e}{1+e_0}\right)^2 - 1\right]\right\} \tag{13}$$

where k_0 is the initial permeability, e_0 is the initial void ratio, and κ and M are non-dimensional material parameters. These parameters used in this study were assumed to be $k_0 = 6\times10^8$ μm^4/N.s, $e_0 = 4$ (Table 1), $\kappa = 0.0848$ and $M = 4.638$ (Holmes & Mow, 1990; Wu & Herzog, 2000), respectively. Figure 4 presents the strain dependent permeability of cell protoplasm and membrane used in ABAQUS software in this study.

Table 1. Material properties of SnHS, PHE and PVHE Models (Ateshian et al., 2007; Wu & Herzog, 2000)

	SnHS		PHE		PVHE	
	Protoplasm	Membrane	Protoplasm	Membrane	Protoplasm	Membrane
Young's modulus E (Pa)	610	10,000	610	10,000	610	10,000
Poisson ratio ν	0.38	0.38	0.38	0.38	0.38	0.38
Shear modulus G_0 (Pa)	235.5	3,623.2	221	3,623.2	221	3,623.2
Prony coefficient g_1	0.4138	0.4138	N/A	N/A	0.31	0.31
Prony coefficient τ_1 (s)	5.2	5.2	N/A	N/A	1.5	1.5
Permeability k_0 ($\mu m^4/N.s$)	N/A	N/A	6×10^8	3000	6×10^8	3000
Void ratio e_0	N/A	N/A	4	3	4	3

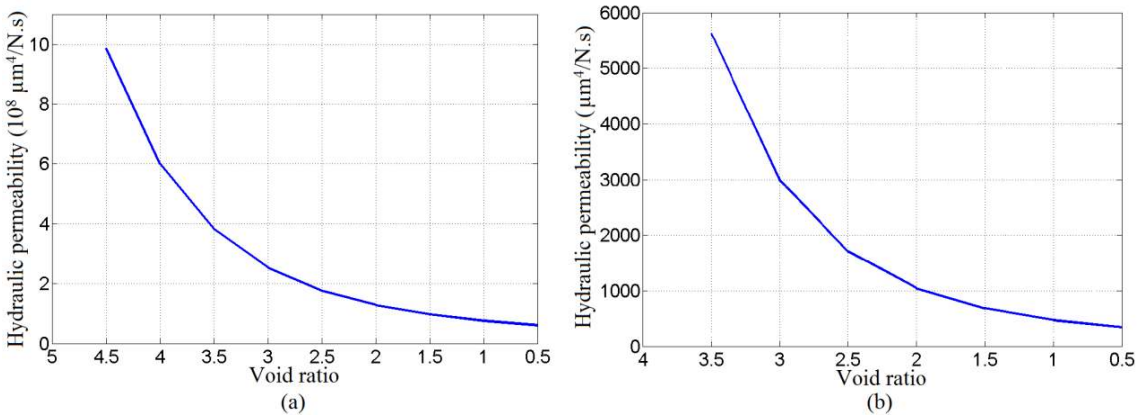

Figure 4 (a) Deformation dependent hydraulic permeability of chondrocyte protoplasm; (b) Deformation dependent hydraulic permeability of chondrocyte membrane

2.2.3. PVHE model

This PVHE model in this study is similar to the PHE model except that the solid component was modeled as Standard Neo-Hookean Solid (SnHS) viscoelasticity (Zhou et al., 2005). However, the SnHS model was modified by using the compressible Neo-Hookean model. The strain energy density function of this compressible material is:

$$W^e = C_1(\bar{I}_1 - 3) + \frac{1}{D_1}(J-1)^2 \quad (14)$$

where C_1 and D_1 are material constants, and J is the volume ratio.

The inverse FEA was conducted to determine the necessary parameters in Eq. 6 and 14 for this PVHE model.

2.3. FEM models

Using three constitutive models discussed in the previous section, two finite element analysis (FEA) models of AFM and micropipette aspiration experiments were developed as stated below. Note that because the mechanical models used in this study are continuum models, which are used to solely identify the bulk mechanical properties of chondrocytes, the cell was assumed to be homogeneous and isotropic for simplification. The macroscale model created in this research provides us with the stress and strain distributions induced on and in the cell which can be utilized as input in the more accurate micro or nanoscale simulation of the cell components i.e. nuclear, and cytoskeleton.

2.3.1. Finite Element Method (FEM) model of AFM experiment

The first FEM model of a single chondrocyte was to study its micro-deformation response by simulating atomic force microscopy (AFM) indentation experiments. The model was created and shown in Figure 5 using commercial software ABAQUS. Because both chondrocyte and AFM tip used are spherical, the axisymmetric element was employed in this study to save computational cost (ABAQUS, 1996). The AFM model consisted of a chondrocyte cell with a diameter of 14 μm, which was indented to a maximum strain of 13% strain (corresponding to a displacement of approximately 1.69 μm). The specimen was indented with a colloidal probe of diameter 5 μm. In order to simulate correctly the AFM experiment, a loading element, namely, i.e., the cantilever base (Figure 5) was created, and connected to the colloidal probe with a spring element of which the spring constant was 0.0217 N/m.

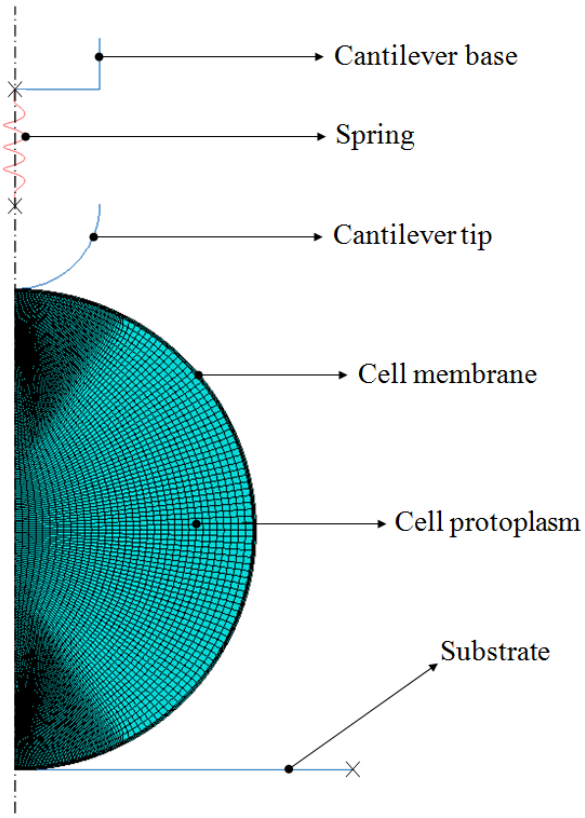

Figure 5 AFM FEM model of single chondrocyte

After indentation, the chondrocyte was allowed to relax for 60 seconds by keeping the displacement of the cantilever constant. Figure 6 presents a typical displacement plot of the cantilever base. All three material models, namely, SnHS, PHE and poroviscohyperelastic (PVHE) were considered and their simulation results were compared to AFM experimental data to investigate the performance of each model. Note that cell membrane was included in FEM models in this study because the stiffness and hydraulic permeability of the cell protoplasm and the membrane are different (Ateshian, Costa, & Hung, 2007; Moo et al., 2012).

After the analysis, the displacements of the cantilever base and the probe were extracted and used to calculate the deflection of the cantilever. The deflection was then multiplied by the spring constant to obtain the force applied to the cell as shown below:

$$F = k_c(d_{base} - d_{bead}) \tag{15}$$

where k_c is the spring constant of the cantilever (e.g 0.0217 N/m in this study), d_{base} and d_{bead} are displacements of the cantilever base and tip, respectively.

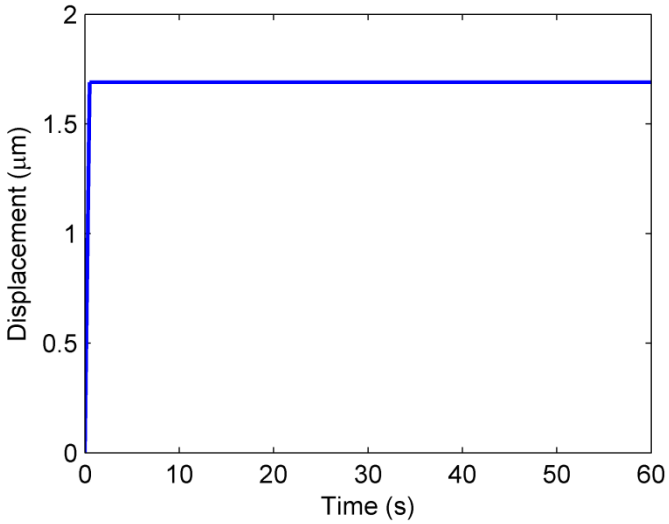

Cantilever base displacement

Time (sec)	Displacement (μm)
0	0
0.5	1.69
60	1.69

Figure 6 Plot of cantilever base movement

2.3.2. FEM model of micropipette aspiration experiment

After validate the models with AFM experiments, an FEM model of single chondrocyte was also developed to simulate the micropipette aspiration experiment to study the creep response of chondrocytes (see Figure 7). This model is similar to that developed in previous study (Zhou et al., 2005) except that the cell membrane was included in this study. The material properties of cell membrane and cell protoplasm for three constitutive models are the same with those of AFM FEM model (see Table 1). This model results were compared to those of two previous works as presented below (Trickey et al., 2000; Zhou et al., 2005).

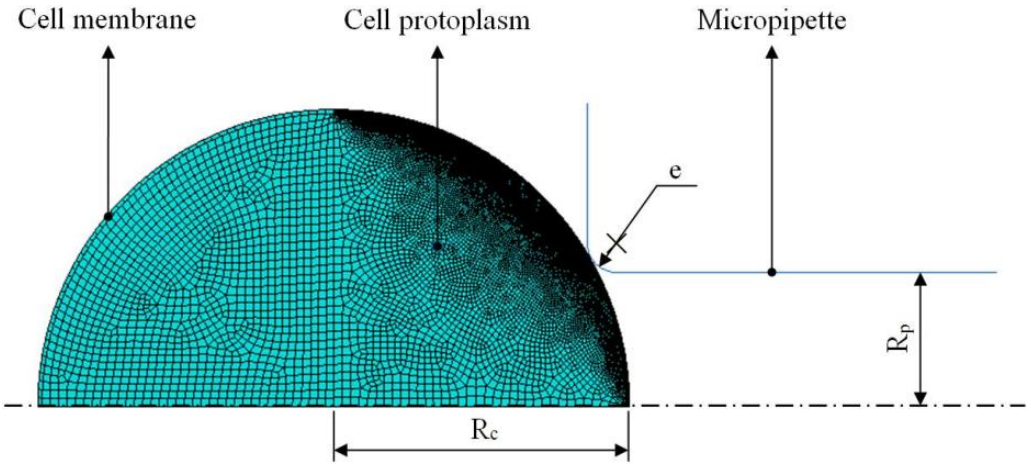

Figure 7 Micropipette aspiration FEM model of single chondrocyte

Firstly in Zhou et al.'s investigation (Zhou et al., 2005), the authors normalized the shear modulus and applied pressure by the shear modulus as well as normalized the geometry dimensions by the initial cell radius R_c. The authors applied the varying normalized pressure $\Delta P/G_0$ of 0.5–2.5 and measured the projection length L_p which was also normalized by the micropipette radius R_p i.e. L_p/R_p. The effect of micropipette radius R_p and fillet radius e were investigated by varying their normalized values (i.e. R_p/R_c and e/R_c) from 0.1 to 0.6 and from 0.02 to 0.1, respectively. It has been concluded that for moderately large pipette ($0.25 \leq R_p/R_c \leq 0.6$), the pipette radius had a much greater influence on the projection length than the fillet radius. Therefore, the normalized micropipette radius of 0.4, 0.45 and 0.5 and the normalized fillet radius of 0.1 were used in this study. Note that the dimensionless approach was not utilized in this study, thus the applied pressure, and pipette radius were varied from 111 to 553 Pa and from 2.84 to 3.55 μm, respectively. The pressure was applied in 0.1 second and kept constant for 5,000 seconds in order to study the creep response of chondrocytes.

Secondly in Trickey et al.'s study (Trickey et al., 2000), the measured shear modulus of chondrocyte was 120 Pa. The cell was applied the pressure difference of 350 Pa which had the normalized value of around 3. Hence, the applied pressure in this study would be around 650 Pa. The pressure was also applied in 0.1 second and kept constant for 5,000 seconds. The projection length extracted in this study will be compared to that published in previous work (Trickey et al., 2000).

III. Results and Discussions

3.1. Analysis of stress relaxation behavior of chondrocytes using AFM experiments and simulations

Firstly, the FEM model of chondrocyte was created to simulate AFM experiment and the simulation results were compared to AFM experimental data to validate the model.

3.1.1. SnHS model

The FEM model was simulated with SnHS material model, in which the chondrocyte was indented to 13% in 0.5 second (see Figure 6) using ABAQUS software. The material parameters are shown in Table 1 and are extracted from AFM experiments. The Mises stress distribution was extracted prior to indentation, after indentation and after relaxation (data not shown). It can be observed that during indentation the stress increased and distributed near the colloidal probe and the substrate and then reduced during relaxation. This is called stress relaxation which is one of the behaviors of viscoelastic materials. The reason of this relaxation behavior is because the cell becomes softer with time i.e. viscoelasticity behavior.

The force-time and force-indentation (F-δ) curves are shown in Figure 8. It can be observed from Figure 8 that the simulation results were similar to AFM experimental results. However, despite the SnHS model can capture the maximum and equilibrium applied forces, the relaxation time is larger than that of experiment. The reason is that the shear relaxation modulus is reduced gradually with time (Zhou et al., 2005). Moreover, this model assumes the cell to be a solid-like material, but it is well-known that the cell consists of both solid skeleton and mobile fluid. Therefore, an FEM model was developed using PHE material and the material properties are the same with those of SnHS model.

3.1.2. PHE model

The PHE model consisted of cell protoplasm, cell membrane, cantilever tip, cantilever base, and substrate (see Figure 5). The protoplasm and membrane's material properties are shown in Table 1, and the rest of components are assumed as rigid bodies. The thickness of the membrane was chosen to be 0.1 μm for numerical stability consideration (Ateshian et al., 2007). The Poisson's ratio was assumed to be same for both protoplasm and membrane. In addition, the hydraulic permeability of membrane was assumed to be 6 orders smaller than that of the protoplasm (Ateshian et al., 2007; Moo et al., 2012). The transient consolidation analysis is used in this study to account for transient effect on cell mechanics. Figure 8 presents the force-time and force-indentation (F-δ) curves extracted from PHE FEM model. As can be seen in Figure 8a, the applied force reached its maximum value and then reduced to its equilibrium value.

This is the effect of volume loss of fluid during relaxation phase. However, this effect is not significant because the maximum value of applied force is different with experimental result. The reason is that hydraulic permeability of cell membrane is much smaller than that of cell protoplasm, which caused the fluid difficult to transport through the membrane. Thus, it is hypothesized that the behaviors of chondrocytes are influenced by not only the interaction between solid and fluid components but also the intrinsic viscoelasticity of solid component (Baaijens et al., 2005; Shieh et al., 2006; Trickey et al., 2006).

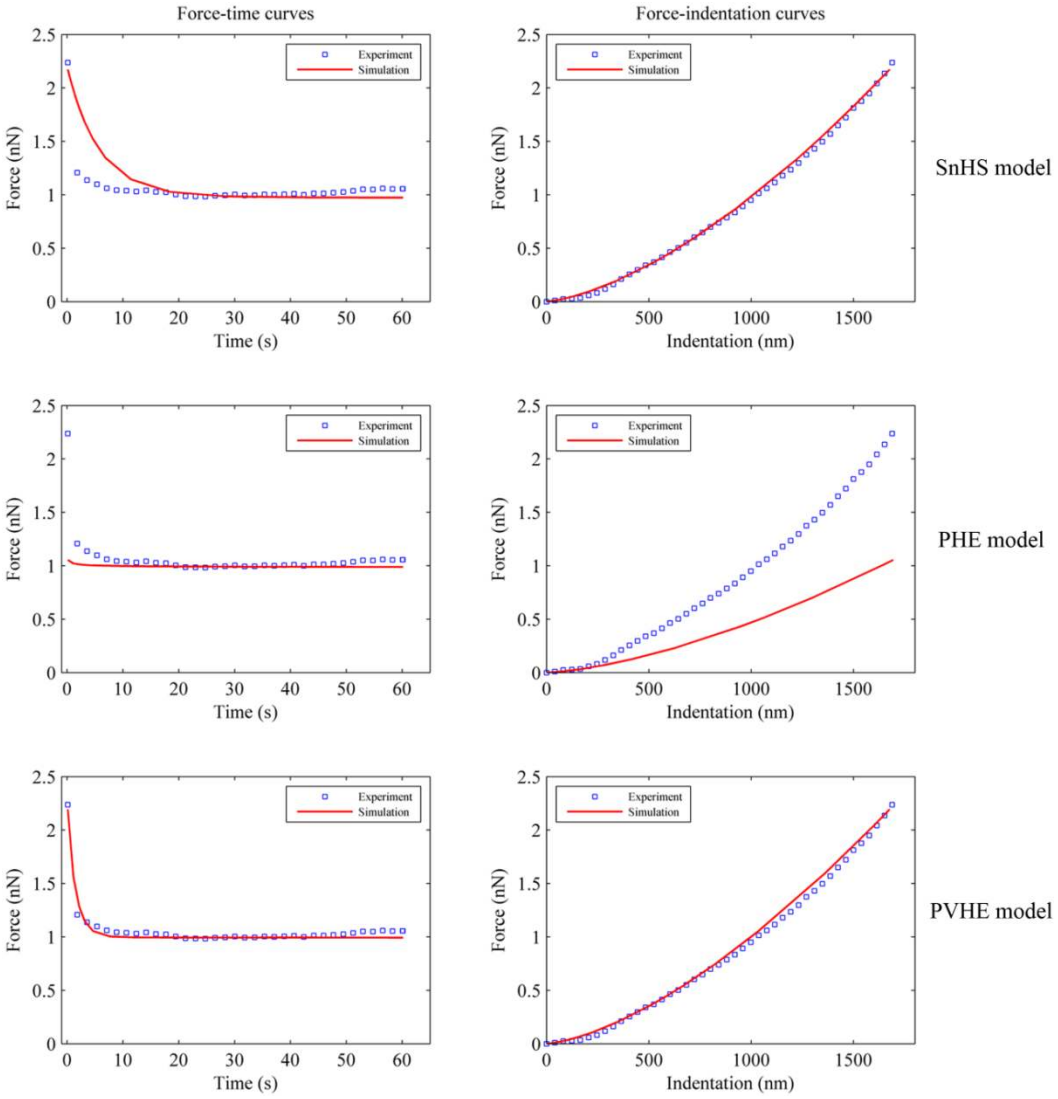

Figure 8 (a) Force-time curves extracted from AFM experiments and from SnHS, PHE and PVHE FEM models; (b) Force-indentation (F-δ) curves extracted from AFM experiments and from SnHS, PHE and PVHE FEM models

Figure 9 presents pore pressure versus time curve measured at the inner membrane node. It can be observed that the fluid pore pressure increased to its maximum value at maximum strain before decaying to its minimum value. These results are similar to those of cartilage as reported in the literature (Oloyede & Broom, 1994; Oloyede et al., 1992). This is the stress sharing mechanism in porous medium where the applied stress is firstly taken by the fluid and then the stress is transferred from fluid to solid in the later stage.

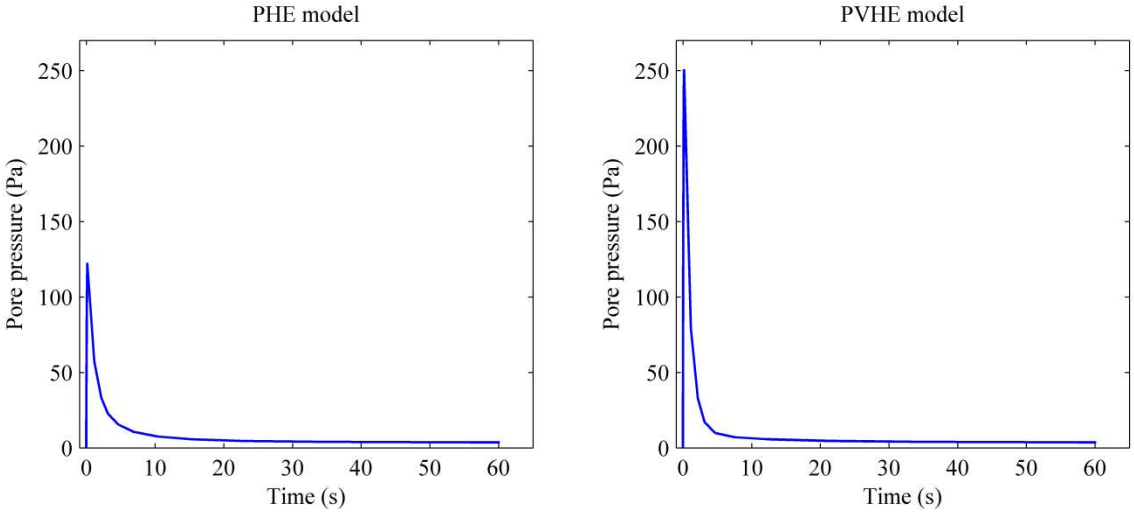

(a) (b)

Figure 9 (a) Pore pressure vs time curve of PHE model; (b) Pore pressure vs time curve of PVHE model

It can be observed from Figure 8a and 9 that during the indentation phase, both applied force and pore pressure reached their maximum value. When the displacement of cantilever tip is kept constant, the difference of pressure between inside and outside of the cell drives the fluid to flow leading to the relaxation behavior. It is demonstrated by the fact that the pore pressure inside the cell decays to zero (see Figure 9) and the applied force reduced to an asymptotical value which is similar to that of SnHS model (see Figure 8a). This relaxation behavior is due to the effect of volume loss of intracellular fluid.

3.1.3. PVHE model

As mentioned above, the mechanical responses of chondrocytes are likely dependent on both fluid-solid interaction and intrinsic viscoelasticity of solid skeleton.

Thus, PVHE model was developed in this study. The protoplasm and membrane's material properties are shown in Table 1, and the rest of components are assumed as rigid bodies. The inverse FEA approach was used to estimate cell viscoelastic properties for this material model (Zhao, Wyss, & Simmons, 2009). The force-time and force-indentation curves, which are shown in Figure 8, had a good agreement with experimental data. It is interesting to note that although SnHS model could simulate stress relaxation response of chondrocyte, the relaxation time was larger than experimental result. In contrast, the PVHE model had a smaller relaxation time which is close to experimental result. This is because the pore fluid responded rapidly and exuded through the membrane right after indentation phase.

Figure 9 shows the pore pressure-time curve which is similar to that of PHE model. The difference is that maximum pore pressure of PVHE model is higher than that of PHE model. This is because the viscohyperelastic material has a larger shear modulus compared to the hyperelastic one in the transient response (Zhou et al., 2005) (see Figure 8).

It can be observed that the PVHE can capture not only the maximum and equilibrium applied forces but also the relaxation time correctly compared to experimental results. Thus, this PVHE model can capture the relaxation behavior better than SnHS and PHE models. Hence, the PVHE model is recommended. Table 2 presents the comparison of maximum force, equilibrium force, and relaxation time of three models.

Table 2. Comparison of three models SnHS, PHE and PVHE

Models	Maximum force (nN)	Equilibrium force (nN)	Relaxation time (s)
SnHS	3.451	2.226	27.2375
PHE	2.521	2.310	15.1875
PVHE	3.460	2.319	15.1875

3.2 Creep response analysis using micropipette aspiration simulation

In order to study the creep response of chondrocyte, the micropipette aspiration experiment was simulated and the simulation results were compared to those of two previous separate experiments. In the first work, the applied pressure was varied from

111 to 553 Pa for each case of the three different pipette radii i.e. 2.84, 3.195 and 3.55 µm. The Mises stress distributions of three models in case of R_p = 2.84 µm and ΔP = 553 Pa were extracted prior to and immediately after pressure application, as well as after creep response (data not shown). It can be observed that the PHE and PVHE models had similar stress distribution, which was slightly different with that of the SnHS model. This is due to the effect of fluid flow.

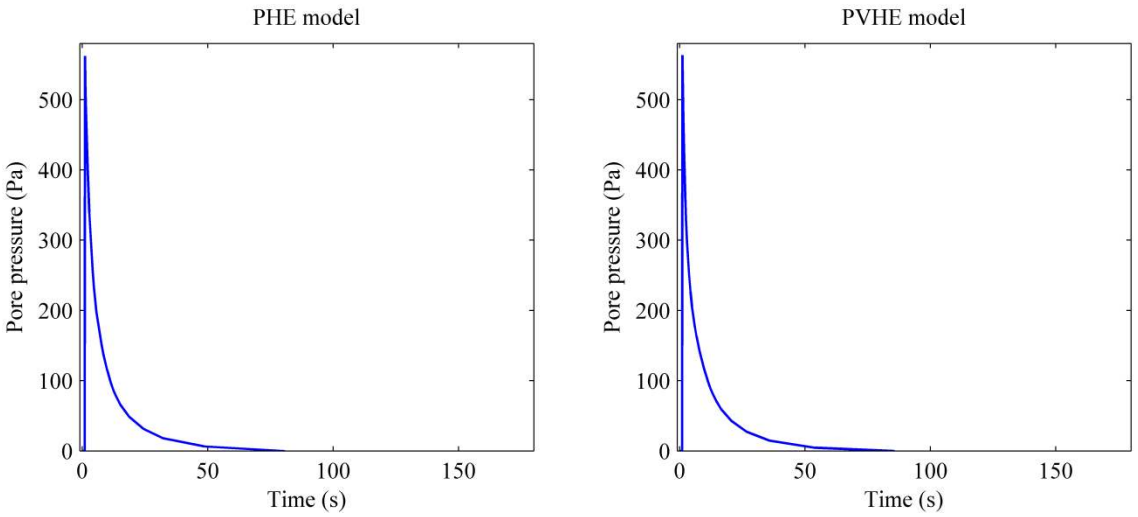

(a) (b)

Figure 10 Pore pressure vs time curves of (a) PHE model and (b) PVHE model in case of R_p = 2.84 µm and ΔP = 553 Pa

The projection length was normalized with pipette radius and compared to that published in previous study (Zhou et al., 2005). Figure 11 shows an effect of pipette radius on elastic force-deformation relationship using PHE and PVHE models. It is worth noting that R_p = 2.84, 3.195 and 3.55 µm in this study is corresponding to R_p* = 0.4, 0.45 and 0.5 in Zhou et al.'s work (Zhou et al., 2005), respectively. It can be observed that all three SnHS, PHE and PVHE models had similar results to each other and to those of previous work except that there was a slightly difference in case of $\Delta P/G_0$ = 2.5.

Recently, Trickey et al. (Trickey et al., 2000) have applied a pressure of ΔP = 350 Pa in their micropipette aspiration experiments and determined the shear modulus of chondrocyte to be G = 120 Pa ($\Delta P/G \approx 3$). Therefore, the second work in this study is that the chondrocyte was applied with a pressure of around 650 Pa (the shear modulus of chondrocyte in this study was G = 221 Pa). The pressure was then kept constant for

180 seconds to investigate chondrocyte's creep response. The projection length of the chondrocyte was extracted and compared to experimental data reported by Trickey et al. (Trickey et al., 2000). Figure 12 presents the project length versus time curves of SnHS, PHE, and PVHE models. It can be observed that all three models can capture the creep response of single chondrocyte. However, the aspiration lengths of chondrocyte at the instant of right before the creep response of three models were different to each other. They were 2.73632, 3.08516 and 2.20406 for SnHS, PHE and PVHE models, respectively. When comparing to experimental result for non-osteoarthritic chondrocyte, the PVHE model captures this behavior better than other two models. Hence, the PVHE model is recommended.

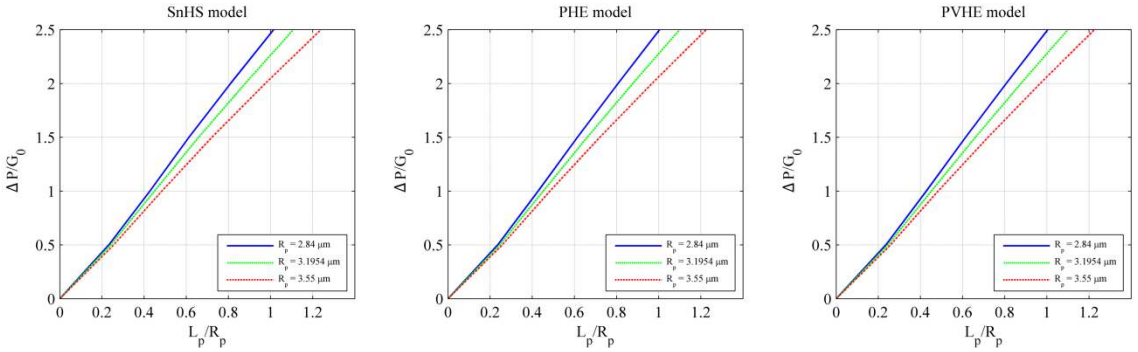

(a) (b) (c)

Figure 11 Effect of pipette radius on elastic force-deformation relationship (a) SnHS model result, (b) PHE model result, and (c) PVHE result

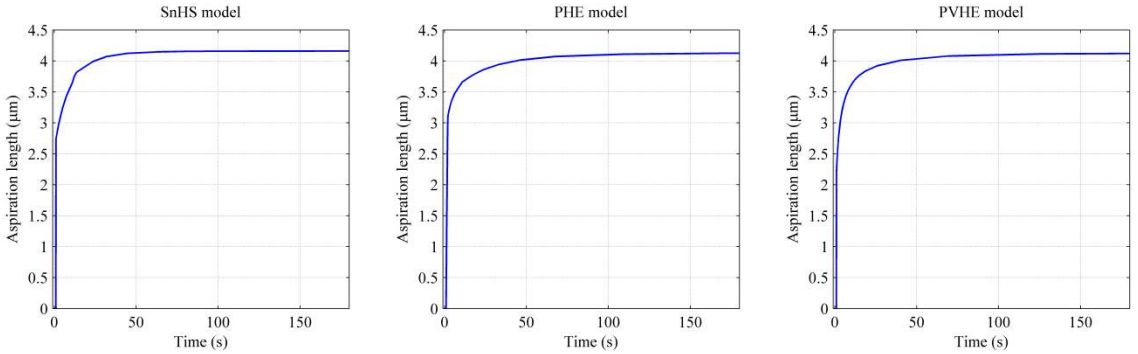

(a) (b) (c)

Figure 12 Aspiration length versus time curves extracted from (a) SnHS model result, (b) PHE model, and (c) PVHE model

IV. Conclusions

This study has developed a poroviscohyperelastic (PVHE) FEM model to simulate AFM and micropipette aspiration experiments of single chondrocyte. The performance of this model is thoroughly compared to that of two other existing models, namely, Standard Neo-Hookean Solid (SnHS) and porohyperelastic (PHE). The following conclusions can be drawn from this study:

- SnHS model is able to capture maximum and equilibrium applied forces of AFM experiment as well as strain-rate-dependent mechanical response of chondrocyte. However, the relaxation time predicted by SnHS is larger than that of experiments.
- Although PHE model could not capture the maximum applied force of AFM experiment, the equilibrium force obtained by PHE agrees well with experimental result. In addition, the relaxation phenomenon due to the effect of volume loss of intracellular fluid could be simulated by using this model based on fluid pore pressure distribution and pore pressure-time curve. This model can also capture the creep response of chondrocyte with slightly difference with micropipette aspiration experimental result.
- PVHE model is more effective than the other two models. The relaxation behavior in this model is because of both viscoelasticity of solid component and stress sharing mechanism between solid and fluid constituents. The maximum and equilibrium applied forces as well as relaxation time predicted by this PVHE model agrees well with AFM experimental results. This model can also capture creep response of chondrocyte in micropipette aspiration experiment very well compared to PHE model. Therefore, this model is strongly recommended.

In brief, the PVHE model has been proven to be the most suitable model for single chondrocyte. This will open a new avenue to explore the biomechanical properties of chondrocytes. In future, other biochemical behaviors of chondrocyte such as swelling behavior will be accounted for in the PVHE model.

Acknowledgement

This research was funded by ARC Future Fellowship project (FT100100172) and QUT Postgraduate Research Scholarship. This work was performed in part at the Queensland node of the Australian National Fabrication Facility (ANFF), a company established under the National Collaborative Research Infrastructure Strategy to provide nano and micro-fabrication facilities for Australia's researchers. The authors would like to thank Dr. Sanjleena Singh for advices in modeling of experiments.

References

ABAQUS. (1996). *ABAQUS/Standard User's Manual (version 5.6)*

Ateshian, G. A., Costa, K. D., & Hung, C. T. (2007). A theoretical analysis of water transport through chondrocytes. *Biomech Model Mechanobiol, 6*, 91-101.

Baaijens, F. P. T., Trickey, W. R., Laursen, T. A., & Guilak, F. (2005). Large Deformation Finite Element Analysis of Micropipette Aspiration to Determine the Mechanical Properties of the Chondrocyte. *Annals of Biomedical Engineering, 33*(4), 494-501.

Biot, M. A. (1941). General Theory of Three-Dimensional Consolidation. *Journal of Applied Physics, 12*, 155-164.

Darling, E. M., Zauscher, S., Block, J. A., & Guilak, F. (2007). A Thin-Layer Model for Viscoelastic, Stress-Relaxation Testing of Cells Using Atomic Force Microscopy: Do Cell Properties Reflect Metastatic Potential. *Biophysical Journal, 92*, 1784-1791.

Darling, E. M., Zauscher, S., & Guilak, F. (2006). Viscoelastic properties of zonal articular chondrocytes measured by atomic force microscopy. *Osteoarthritis and Cartilage, 14*, 571-579.

Faria, E. C., Ma, N., Gazi, E., Gardner, P., Brown, M., Clarke, N. W., & Snook, R. D. (2008). Measurement of elastic properties of prostate cancer cells using AFM. *Analyst, 133*, 1498-1500.

Franz, C. M., & Puech, P. H. (2008). Atomic force microscopy: a versatile tool for studying cell morphology, adhesion and mechanics. *Cellular and Molecular Bioengineering, 1*(4), 289-300.

Higginson, G. R., & Norman, R. (1974). The Lubrication of Porous Elastic Solids with Reference to the Functioning of Human Joints. *Journal of Mechanical Engineering Science, 16*(4), 250-257.

Holmes, M. H., & Mow, V. C. (1990). The nonlinear characteristics of soft gels and hydrated connective tissues in ultrafiltration. *Journal of Biomechanics, 23*(11), 1145-1156.

Jones, W. R., Ting-Beall, H. P., Lee, G. M., Kelley, S. S., Hochmuth, R. M., & Guilak, F. (1997). *Mechanical Properties of Human Chondrocytes and Chondrons from*

Normal and Osteoarthritic Cartilage. Paper presented at the 43rd Annual Meeting, Orthopaedic Research Society, San Francisco, California.

Kaufmann, M. V. (1996). *Porohyperelastic Analysis of Large Arteries Including Species Transport and Swelling Effects.* (Ph. D. Dissertation), The University of Arizona, Tucson, AZ.

Kuznetsova, T. G., Starodubtseva, M. N., Yegorenkov, N. I., Chizhik, S. A., & Zhanov, R. I. (2007). Atomic force microscopy probing of cell elasticity. *Micron, 38*, 824-833.

Lin, D. C., Dimitriadis, E. K., & Horkay, F. (2007). Elasticity of rubber-like materials measured by AFM nanoindentation. *eXPRESS Polymer Letters, 1*(9), 576-584.

McCutchen, C. W. (1982). Cartilage is poroelastic, not viscoelastic (including and exact theorem about strain energy and viscous loss, and an order of magnitude relation for equilibration time). *Journal of Biomechanics, 15*(4), 325–327.

McCutchen, C. W. (1998). Consolidation theory derived without invoking porosity. *International Journal of Solids and Structures, 35*(1-2), 69–81.

Meroi, E. A., Natali, A. N., & Schrefler, B. A. (1999). A Porous Media Approach to Finite Deformation Behaviour in Soft Tissues. *Computer Methods in Biomechanics and Biomedical Engineering, 2*, 157-170.

Moo, E. K., Herzog, W., Han, S. K., Abu Osman, N. A., Pingguan-Murphy, B., & Federico, S. (2012). Mechanical behaviour of in-situ chondrocytes subjected to different loading rates: a finite element study. *Biomech Model Mechanobiol, 11*, 983-993.

Mow, V. C., Kuei, S. C., Lai, W. M., & Armstrong, C. G. (1980). Biphasic creep and stress relaxation of articular cartilage in compression_Theory and experiments. *Journal of Biomechanical Engineering, 102*(1), 73-84.

Mow, V. C., Ratcliffe, A., & Poole, A. R. (1992). Cartilage and diarthrodial joints as paradigms for hierarchical materials and structures. *Biomaterials, 13*(2), 67-97.

Nguyen, T. C. (2005). *Mathematical Modelling of the Biomechanical Properties of Articular Cartilage.* (PhD. Thesis), Queensland University of Technology, Brisbane, Australia.

Oloyede, A., & Broom, N. D. (1991). Is classical consolidation theory applicable to articular cartilage deformation? *Clinical Biomechanics, 6*(4), 206–212.

Oloyede, A., & Broom, N. D. (1994). The Generalized Consolidation of Articular Cartilage: An Investigation of Its Near-Physiological Response to Static Load. *Connective Tissue Research, 31*(1), 75-86.

Oloyede, A., & Broom, N. D. (1996). The Biomechanics of Cartilage Load-Carriage. *Connective Tissue Research, 34*(2), 119-143.

Oloyede, A., Flachsmann, R., & Broom, N. D. (1992). The Dramatic Influence of Loading Velocity on the Compressive Response of Articular Cartilage. *Connective Tissue Research, 27*, 211-224.

Rico, F., Roca-Cusachs, P., Gavara, N., Farre, R., Rotger, M., & Navajas, D. (2005). Probing mechanical properties of living cells by atomic force microscopy with blunted pyramidal cantilever tips. *Physical Review E, 72*(021914), 1-10.

Sherwood, J. D. (1993). Biot poroelasticity of a chemically active shale. *Proc. R. Soc. Lond. A, 440*, 365-377.

Shieh, A. C., Koay, E. J., & Athanasiou, K. A. (2006). Strain-dependent recovery behavior of single chondrocytes. *Biomechan Model Mechanobiol, 5*, 172-179.

Simon, B. R. (1992). Multiphase Poroelastic Finite Element Models for Soft Tissue Structures. *Applied Mech. Rev., 45*(6), 191-219.

Simon, B. R., & Gaballa, M. A. (1989). Total Lagrangian 'porohyperelastic' finite element models of soft tissue undergoing finite strain.pdf. *1989 advances in bioengineering, B Rubinsky (ed), BED-vol 15, ASME, New York*, 97-98.

Simon, B. R., Kaufmann, M. V., McAfee, M. A., & Baldwin, A. L. (1998). Porohyperelastic finite element analysis of large arteries using ABAQUS. *ASME Journal of Biomechanical Engineering, 120*, 296-298.

Simon, B. R., Kaufmann, M. V., McAfee, M. A., Baldwin, A. L., & Wilson, L. M. (1998). Identification and Determination of Material Properties for Porohyperelastic Analysis of Large Arteries. *ASME Journal of Biomechanical Engineering, 120*, 188-194.

Simon, B. R., Liable, J. P., Pflaster, D., Yuan, Y., & Krag, M. H. (1996). A Poroelastic Finite Element Formulation Including Transport and Swelling in Soft Tissue Structures. *Journal of Biomechanical Engineering, 118*, 1-9.

Singh, S., Jones, B. J., Crawford, R. W., & Xiao, Y. (2008). Characterization of a mesenchymal-like stem cell population from osteophyte tissue. *Stem cells and development, 17*(2), 245-254.

Terzaghi, K. (1943). *Theoritical Soil Mechanics*: John Wiley, New York.

Touhami, A., Nysten, B., & Dufrene, Y. F. (2003). Nanoscale mapping of the elasticity of microbial cells by atomic force microscopy. *Langmuir, 19*, 4539-4543.

Trickey, W. R., Baaijens, F. P. T., Laursen, T. A., Alexopoulos, L. G., & Guilak, F. (2006). Determination of the Poisson's ratio of the cell: recovery properties of chondrocytes after release from complete micropipette aspiration. *Journal of Biomechanics, 39*(1), 78-87.

Trickey, W. R., Lee, G. M., & Guilak, F. (2000). Viscoelastic Properties of Chondrocytes from Normal and Osteoarthritic Human Cartilage. *Journal of Orthopaedic Research, 18*, 891-898.

Wu, J. Z., & Herzog, W. (2000). Finite Element Simulation of Location- and Time-Dependent Mechanical Behavior of Chondrocytes in Unconfined Compression Tests. *Annals of Biomedical Engineering, 28*, 318–330.

Zhang, C. Y., & Zhang, Y. W. (2007). Effects of membrane pre-stress and intrinsic viscoelasticity on nanoindentation of cells using AFM. *Philosophical Magazine, 87*(23), 3415-3435.

Zhao, R., Wyss, K., & Simmons, C. A. (2009). Comparison of analytical and inverse finite element approaches to estimate cell viscoelastic properties by micropipette aspiration. *Journal of Biomechanics, 42*, 2768–2773.

Zhou, E. H., Lim, C. T., & Quek, S. T. (2005). Finite Element Simulation of the Micropipette Aspiration of a Living Cell Undergoing Large Viscoelastic Deformation. *Mechanics of Advanced Materials and Structures, 12*(6), 501-512.